Int. J. High Technology Ceramics **1** (1985) 87–105

Creep of Reaction-bonded, Siliconized Silicon Carbide

H. Cohrt and F. Thümmler

Institut für Werkstoffkunde II, Universität Karlsruhe,
Institut für Material- und Festkörperforschung, Kernforschungszentrum Karlsruhe,
Postfach 3640, D-7500 Karlsruhe 1, FRG

SUMMARY

Creep of reaction-bonded siliconized silicon carbide (SiSiC) has been found to be of a transient nature under most of the experimental conditions, and can be described by an extended Norton creep law, considering strain-hardening processes. The deformation is controlled by the silicon carbide skeleton that limits the deformation. A steady-state creep component of the creep curve, observed only under certain conditions, seems to be correlated with microstructural damage. The damaging process can be divided into two stages, microcrack formation and microcrack growth, the latter leading also to pore formation. Creep rupture occurs only above a threshold stress.

1. INTRODUCTION

Of the technical ceramics, those based on silicon carbide and silicon nitride have reached the greatest potential for use at high temperatures. A special silicon carbide material is the reaction-bonded, siliconized silicon carbide (SiSiC). The evaluation of this material has reached a standard which allows its successful use as a structural material at temperatures up to 1350 °C, for example for combustion chambers, components of gas-turbines, heat exchangers, evaporators, thermally stressed rollers, and rocket nozzles.

SiSiC is a two-phase ceramic material consisting of up to 95% silicon carbide, and free silicon in the range 5–40%. The density varies from 3·17–2·86 $Mg\,m^{-3}$ with variation in the content of free silicon. At the present time 25 °C bend strength values of 350–400 M Pa can be reached. The good thermal conductivity and the low thermal expansion result in good

Int. J. High Technology Ceramics 0267-3762/85/$03·30

TABLE 1
Literature Results Dealing with Creep of SiSiC

Author	*Year of publication*	*Test parameter*		*Atmosphere*	*Results*	*Reference*
		Temperature/ °C	*Stress/ MPa*			
P. Marshall	1967	1 000–1 360	290	Carbon dioxide	Transient creep according to $\varepsilon \sim t^{1/3}$, grain boundary sliding influenced by free silicon	1
J. C. V. Rumsey and A. L. Roberts	1967	1 200	140–170	Air	Stationary creep, creep mechanism influenced by free silicon	2
P. Marshall and R. B. Jones	1969	1 000–1 200	207–414	Air	Transient creep according to $\varepsilon \sim t^k$, $k = 0{\cdot}2$–$0{\cdot}5$	3
R. M. Adams	1972	Tensile test		—	Stationary creep, $\dot{\varepsilon}_s \sim \sigma^n$, $n = 1$	4
N. J. Osborne	1975	1 227–1 370	77	Air	No statement on creep mechanisms	5
M. Seltzer	1976	1 400	110–138	Air	No statement on creep mechanisms	6
V. Krishnamachari and M. R. Notis	1977	1 300–1 400	34–86	Air	Grain boundary diffusion controlled by silicon-diffusion	7
D. C. Larsen *et al.*	1978	1 200	240–275	Air	No statement on creep mechanisms	8
G. Wirth *et al.*	1978	1 200	1 200	Air	No statement on creep mechanisms	9
		Tensile test				
K. Schnürer *et al.*	1979 1980	810–1 200	100–190	Air and vacuum	Grain boundary diffusion controlled by silicon diffusion and dislocation mechanisms within the silicon carbide grains	10 11
E. Gugel *et al.*	1981	1 200–1 350	130–190	Air	No final statement on creep mechanisms	12
C. H. Carter *et al.*	1984	1 575–1 650	110–220	Air	Stationary creep, $\dot{\varepsilon}_s \sim \sigma^n$, $n = 5{\cdot}7$ Dislocation climb within silicon carbide grains	13
		Compression test				

thermal shock resistance. The inherent good oxidation resistance of the constituents results in good oxidation behaviour of SiSiC.

In looking at creep behaviour, large differences in the interpretations of the results are seen. A comprehensive overview of the papers dealing with creep of SiSiC is given in Table 1. In this work the creep behaviour of SiSiC is reinvestigated and attention is drawn to the deformation mechanisms. The process of creep damage is also discussed.

2. MATERIALS

The investigations were carried out on two materials produced by slip casting. The main features of the materials are given in Table 2. Free carbon was found to be the main impurity but with a total content of not

TABLE 2
Content of Free Silicon and Density of the SiSiC Materials

Material	*Free silicon*		*Density* ρ/*Mg m*$^{-3}$	
	(*Vol.* %)	(*wt* %)	ρ_1[a]	ρ_2[b]
1	15·5	11·7	3·03	3·08
2	14·5	11·0	3·08	3·09

[a] Determined by weighing.
[b] Determined by image analysis.

more than 0·5 %. Other impurities were found only in small quantities (i.e. Fe < 0·1 %, Ca < 0·05 %, Mg < 0·01 %, Al < 0·1 %, B < 0·1 %). These impurities were detected by wet chemical methods. Oxygen was not found by Auger-electronspectroscopy if the sample had been sputtered by argon ions during the measurement. Therefore the material can be regarded as being substantially free of oxygen.

The microstructures of the materials are shown in Fig. 1. The polished specimens were etched by Murakami's solution (100 ml water, 10 g sodium hydroxide, 10 g potassium ferricyanide). The silicon carbide is the grey phase and the free silicon is the white one. In material 1 large dark areas are seen, consisting of porous free carbon which did not react during processing. The porous free carbon is the reason for the great difference between the measured and calculated densities in Table 2. The silicon carbide phase usually consists of primary and secondary silicon carbide, the latter being formed by the reaction of carbon and silicon during infiltration of the preform.

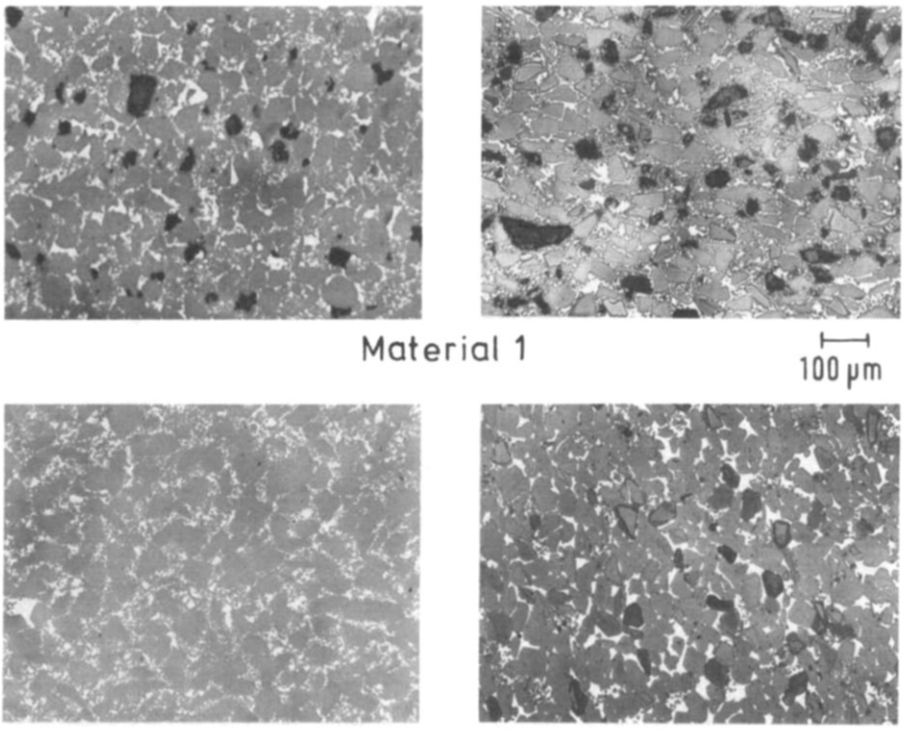

Fig. 1. Microstructure of the SiSiC materials. Left, unetched; right, etched by Murakami's solution.

By etching, boundaries within the silicon carbide structure become visible which makes possible a distinction between the coarse- and fine-grained primary silicon carbide and the secondary silicon carbide. It is not easy to distinguish between the fine-grained primary and the secondary silicon carbide.

By ceramographic investigation four typical defects in the microstructure of SiSiC were found (Fig. 2). The most frequent defects, especially in Material 1, were particles of free porous carbon (Fig. 2(a)) which were surrounded by a dense barrier of silicon carbide formed during the infiltration process. The silicon carbide barrier prevents the diffusion processes needed for transformation of the free carbon into secondary silicon carbide.

Sometimes large areas of free silicon were found in the microstructure (Fig. 2(b)). These defects may be due to bubbles in the slip which could not escape during preparation of the preform and were filled by free silicon during the infiltration process.

Cracks in the silicon carbide structure should be regarded as very critical

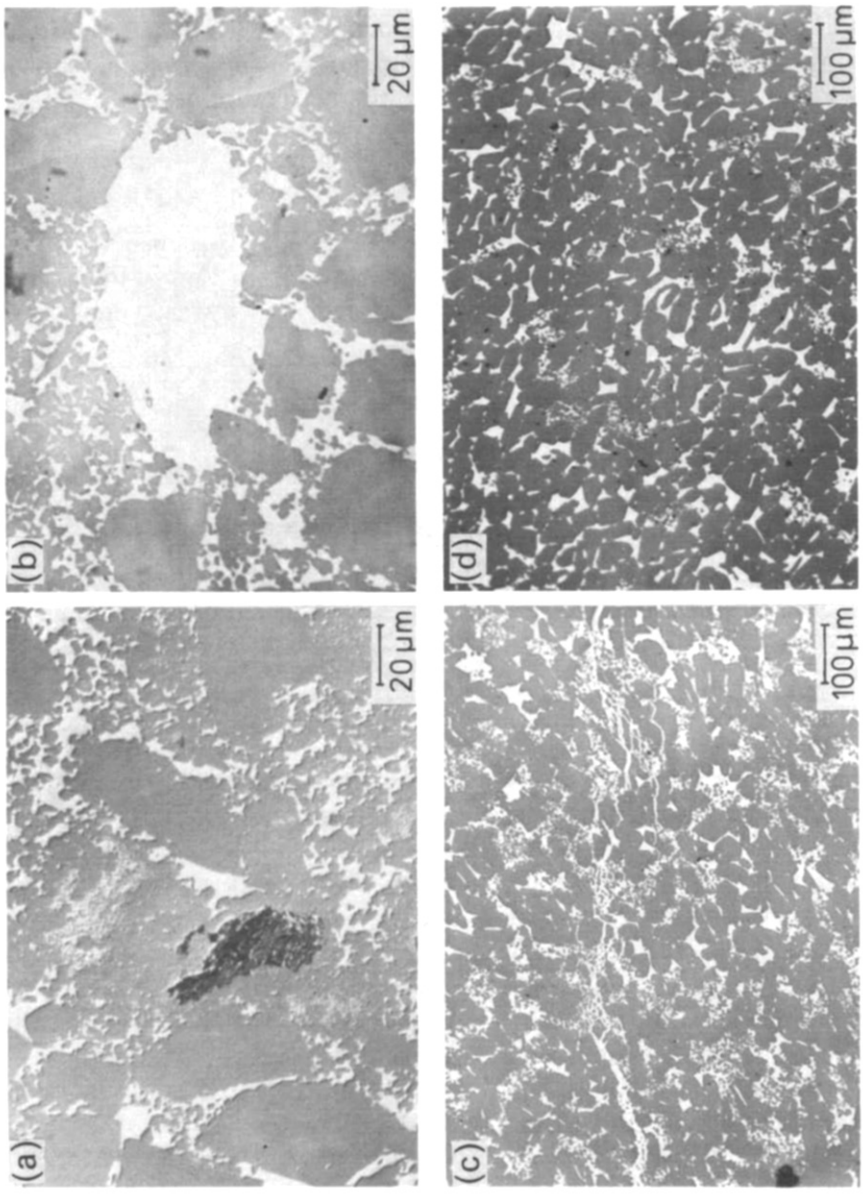

Fig. 2. Microstructure defects in SiSiC. (a) Inclusion of free carbon (Material 1); (b) large area of free silicon (Material 1); (c) crack in the silicon carbide structure filled by free silicon (Material 1); (d) inhomogeneous distribution of fine-grained silicon carbide (Material 2).

defects (Fig. 2(c)). These cracks can be initiated by the anomalous solidification behaviour of the free silicon, which shows, analogous to water, an expansion of about 10% by volume during solidification. The cracks sometimes reach a length of several millimetres and large silicon carbide grains can be made to split. Generally the cracks were filled with free silicon.

The inhomogeneous distribution of the fine-grained silicon carbide shown in Fig. 2(d) may be regarded as a further microstructure defect.

3. EXPERIMENTAL DETAILS

The creep tests were carried out on a 4-point bend specimen with the dimensions 4·5 mm × 3·5 mm × 45 mm. The main dimensions of the fixture are given in Fig. 3. The diameter of the rollers (d) was 3 mm. This

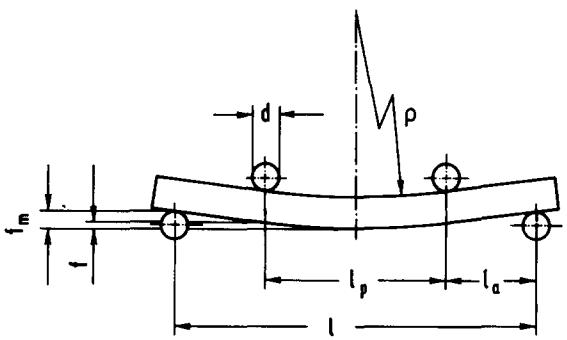

Fig. 3. Dimensions of the bend creep fixture ($l = 40$ mm, $l_a = 10$ mm, $l_p = 20$ mm, $d = 3$ mm).

configuration was taken as the standard for the bend test in the German research programme 'Keramische Komponenten für die Fahrzeug-Gasturbine'. To prevent any detrimental influence of the edges, these were provided with a 45°-bevel. The specimens were carefully ground along the direction of the long specimen axis.

The furnace was heated by a resistance heater and the temperature was controlled within the range of ±2 °C. The strain was measured as the deflection in the middle of the specimen by a linear variable displacement transducer (LVDT). Using the assumption of the theory of Bernoulli (i.e. plane cross-sections remain plane during creep), the strain, ε, of the outer tensile fibre can be calculated:

$$\varepsilon = \frac{2\rho}{h} = \frac{4h}{l_p^2} f \tag{1}$$

where ρ = radius of curvature of the neutral axis and h is the beam thickness (= 3·5 mm). For the definition of the other symbols see Fig. 3. The used

fixture allows only the measurement of the total deflection f_m. For this reason the interdependence:

$$\frac{f}{f_m} = 1 - 4\frac{l_a}{l} \cdot \frac{1 - \frac{4}{3}\frac{l_a}{l}}{1 - \frac{4}{3}\left(\frac{l_a}{l}\right)^2} \tag{2}$$

has to be taken into account.

For the calculation of the stress the linear elastic theory is used. The nominal stress of the outer fibres, σ_n, within the range of the inner rollers (range of constant moment) is:

$$\sigma_n = \frac{M}{W} \tag{3}$$

where M = bending moment and W = moment of resistance. The linear elastic theory is applied in spite of the well-known fact that the stress distribution within the bending specimen becomes nonlinear with time if the creep law is nonlinear (i.e. the power law of creep $\dot{\varepsilon} \sim \sigma^n, n > 1$ (Ref. 14)). In the nonlinear case the stress distribution depends on time and on the creep law itself; this fact is not generally known. Thus it seems to be convenient to operate with the linear elastic theory and to characterize the applied stress by the nominal stress, σ_n, of the outer fibres according to eqn (3).

In order to investigate the influence of oxidation effects on the creep of SiSiC the tests were carried out on specimens in the as-received state and on preoxidized materials. The preoxidation conditions were chosen to be 1350 °C and 200 h, in air.

4. RESULTS

All measured creep curves showed a decreasing creep rate, even under severe test conditions, after long test times up to 400 h. This is in good agreement with earlier publications.[1,3] Due to this fact it is not possible to characterize the creep mechanisms in a simple way by application of stationary creep rates. Creep of SiSiC is mainly of a transient nature.

To describe the creep curve of tin in 1911 Andrade[15] suggested the equation:

$$l(t) = l_0(1 + \beta' t^{1.3})\, e^{kt} \tag{4}$$

where $l(t)$ is the length of the specimen as a function of time t, l_0 is the initial length, and β' and k are constants. This equation was modified by Cottrell and Aytekin[16] who introduced a stationary creep rate, $\dot{\varepsilon}_s$:

$$\varepsilon(t) = \varepsilon_0 + \beta' t^{1.3} + \dot{\varepsilon}_s t \tag{5}$$

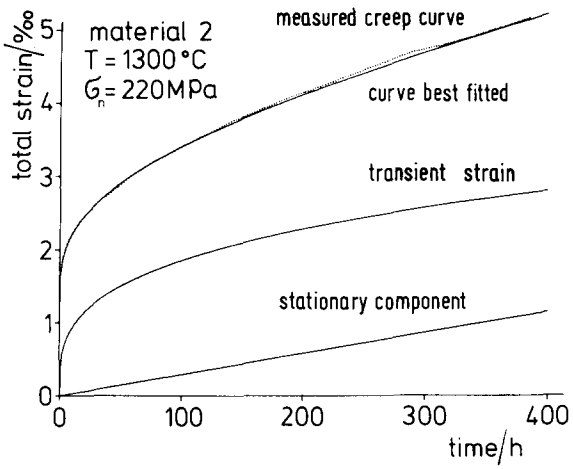

Fig. 4. Creep curve of SiSiC and comparison of measured curve with the curve best fitted.

where $\varepsilon(t)$ is the total strain, ε_0 is an instantaneous strain and $\beta' t^{1/3}$, with the constant β', is a transient strain. From eqn (5), with a general time exponent m and the dimensionless time (t/t_0), the strain–time relation can be written:

$$\varepsilon(t) = \varepsilon_0 + \beta\left(\frac{t}{t_0}\right)^m + \dot{\varepsilon}_s t \tag{6}$$

This equation describes the creep curve very well (Fig. 4). The parameters ε_0, β, m and $\dot{\varepsilon}_s$ can be calculated by a computer program using linear regression analysis.[17] From Fig. 4 it is seen that even at 400 h the contribution of transient strain to the total strain is significantly higher than the contribution of stationary strain $\dot{\varepsilon}_s t$. The strain rates indicated by the slope of the curves are of the same order for the transient and the stationary part of strain at this point.

Measurable stationary strain rates of the order of $\dot{\varepsilon}_s > 10^{-6}\,\mathrm{h}^{-1}$ could only be found in Material 1 under all test conditions. In Material 2 stationary strain rates could only be measured when the silicon carbide structure was damaged by cracks as in Fig. 2(c), or in cases of very severe test conditions.

For SiSiC a large scatter in the parameters of the creep curve is obtained.[17] For this reason a more complicated dependence of the parameters of transient creep on the nominal stress, σ_n, other than linearity, can not be seen. The method of least squares leads to an equation of the form:

$$y = (a \pm l_a) + (b \pm l_b)x \tag{7}$$

The constants a and b are supplemented by the 90%-confidence regions l_a

and l_b. The creep curve of SiSiC was measured at the following stress levels: 130, 160, 190 and 220 MPa.

Each measurement was repeated five times at a temperature of 1300 °C. Using this procedure the following dependences are found for the parameter describing the initial strain, ε_0, and the parameters for transient creep, β and m, for Material 1:

$$\begin{aligned}
\varepsilon_0[‰] &= -(0{\cdot}396 \pm 0{\cdot}136) + (8{\cdot}58 \pm 3{\cdot}52) \times 10^{-3}\sigma_n\ [\mathrm{MPa}] \\
\beta[‰] &= (0{\cdot}552 \pm 0{\cdot}033) - (1{\cdot}89 \pm 0{\cdot}84) \times 10^{-3}\sigma_n\ [\mathrm{MPa}] \\
m[1] &= (0{\cdot}034 \pm 0{\cdot}044) + (1{\cdot}39 \pm 1{\cdot}04) \times 10^{-3}\sigma_n\ [\mathrm{MPa}]
\end{aligned} \tag{8a}$$

and for Material 2:

$$\begin{aligned}
\varepsilon_0[‰] &= -(0{\cdot}151 \pm 0{\cdot}032) + (6{\cdot}32 \pm 2{\cdot}49) \times 10^{-3}\sigma_n\ [\mathrm{MPa}] \\
\beta[‰] &= (0{\cdot}448 \pm 0{\cdot}067) - (1{\cdot}31 \pm 1{\cdot}18) \times 10^{-3}\sigma_n\ [\mathrm{MPa}] \\
m[1] &= (0{\cdot}074 \pm 0{\cdot}035) + (1{\cdot}49 \pm 0{\cdot}62) \times 10^{-3}\sigma_n\ [\mathrm{MPa}]
\end{aligned} \tag{8b}$$

For Material 1 a stationary strain component which showed a large scatter was obtained at all test conditions. The results are plotted in the log–log plot shown in Fig. 5. From this diagram a stress exponent of $n = 5 \pm 1{\cdot}5 (\dot{\varepsilon}_s \sim \sigma^n)$ can be calculated by the method of least squares. For Material 2 such a diagram is not meaningful because stationary strain rates were obtained only at stress levels higher than 220 MPa.

The question arises as to at which stress level creep rupture occurs. On Material 1 at 1300 °C a nominal stress of 190 MPa could be applied without creep rupture within 200 h. But a nominal stress of 213 MPa ($\approx 70\%$ of

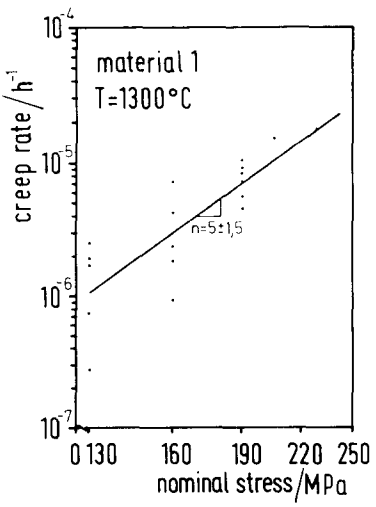

Fig. 5. Stress dependency of the stationary strain component.

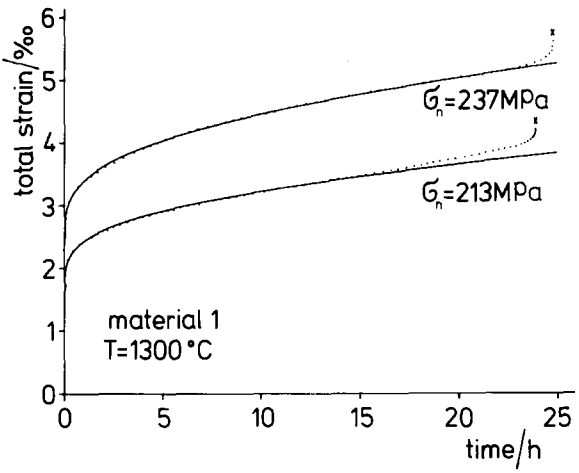

Fig. 6. Complete creep curve of SiSiC at very high stresses.

room temperature strength) led to creep rupture within 24 h (Fig. 6). The creep curves then show extensive tertiary creep before creep rupture occurs. From this creep curve a stationary creep rate of $\dot{\varepsilon} \approx 1{\cdot}5 \times 10^{-5}\,h^{-1}$ can be calculated by the procedure mentioned above. These creep rates are also plotted in Fig. 5. They are very well integrated in the band of scatter.

An interesting change in the creep mechanisms can be demonstrated by plotting the plastic strain, $\varepsilon_{pl} = \beta(t/t_0)^m + \dot{\varepsilon}_s t$, versus the nominal stress for different constant creep times (Fig. 7). It becomes clear that within the scattering band the strain at a constant time is independent of the stress for low nominal stresses, while at high stresses the strain increases significantly. The critical stress shifts to lower nominal stresses with increasing time at

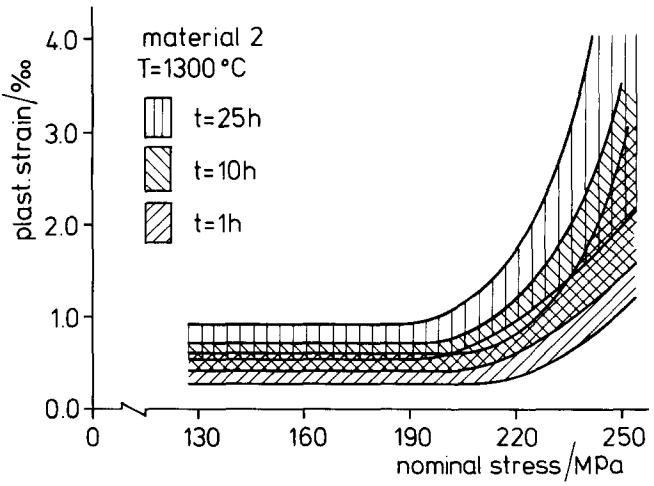

Fig. 7. Plastic strain versus nominal stress at different constant creep times.

TABLE 3
Comparison of the Parameters of Instantaneous and Transient Strain in the As-received and Preoxidized States

	$\varepsilon_0/‰$	$\beta/‰$	m/l
As-received state	$0{\cdot}810 \pm 0{\cdot}229$	$0{\cdot}213 \pm 0{\cdot}126$	$0{\cdot}182 \pm 0{\cdot}063$
Preoxidized 1 350 °C, 200 h	$0{\cdot}717 \pm 0{\cdot}247$	$0{\cdot}222 \pm 0{\cdot}078$	$0{\cdot}168 \pm 0{\cdot}044$

which the strain was taken. This finding indicates a necessary incubation time for reaching large strain values. The incubation time is lower the higher the nominal stress.

For determining the influence of oxidation on the creep of SiSiC, tests were carried out on Material 2 in the as-received state and in the preoxidized state. Table 3 gives the mean values and standard deviation of the instantaneous strain and the parameters of transient strain. The comparison shows no significant differences. This means that a severe oxidation treatment before creep testing does not influence the creep behaviour and the influence of oxidation on creep of SiSiC can, in general, be disregarded.

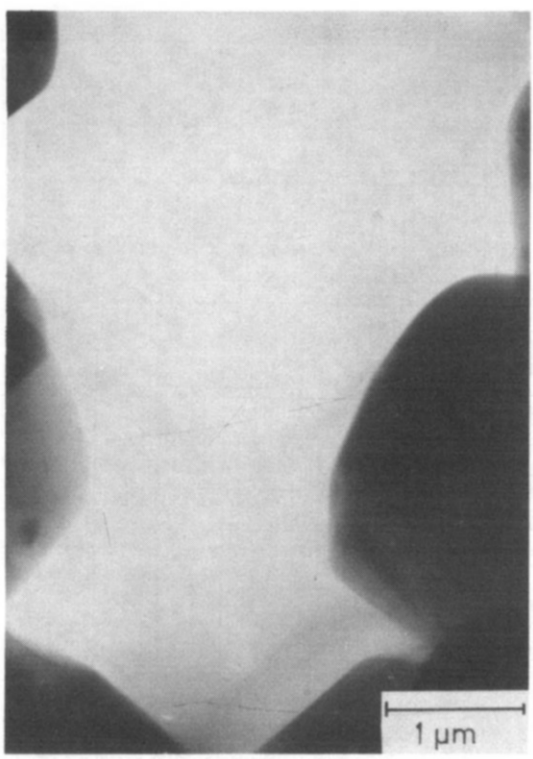

Fig. 8. TEM micrograph of Material 2 in the as-received state; silicon region free of any dislocation.

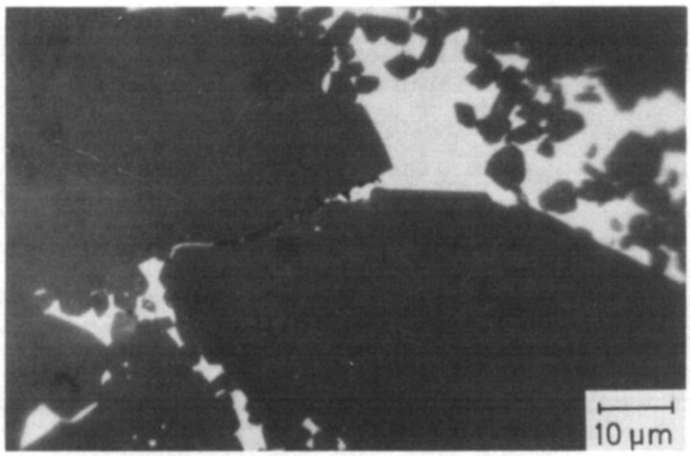

Fig. 9. Optical micrograph of Material 2 after 50 h creep at 1300 °C and 220 MPa.

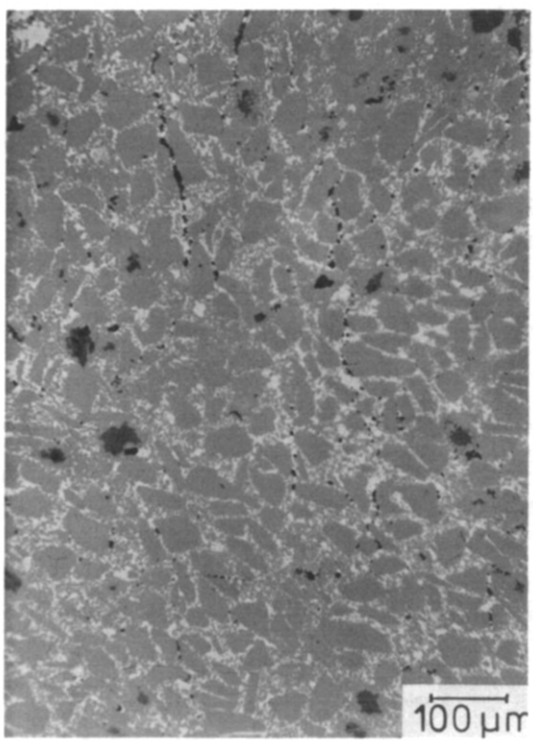

Fig. 10. Optical micrograph of Material 1 after 200 h creep at 1350 °C and 190 MPa.

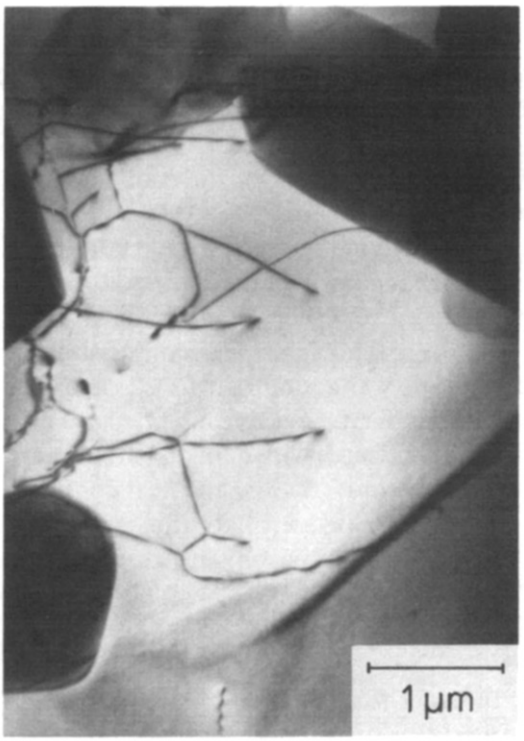

Fig. 11. TEM micrograph of silicon regions in Material 2 after 400 h creep at 1300 °C and 220 MPa.

Investigations by light microscopy and transmission electron microscopy (TEM) discovered some significant changes in the microstructure due to creep. In the as-received state no defects of microstructure other than those mentioned above could be discerned by light microscopy and only a few dislocations were found by TEM in the silicon carbide and silicon phases. In Fig. 8 a large region of free silicon, free of any dislocation, is shown. After a creep test when no stationary creep according to eqn (6) occurs, in general no influence of creep on the microstructure can be detected by light microscopy. In other cases microcracks appear between silicon carbide grains with grain boundaries perpendicular to the direction of the tensile stress (Fig. 9). In the later creep state the microcracks form pores which are arranged in planes also perpendicular to the direction of tensile stress (Fig. 10). After all creep tests a significant number of dislocations and twins were found in the silicon phase (Fig. 11). No change could be detected, however, in the configuration of dislocations in the silicon carbide grains. Cracks and pores were also found by TEM studies but it was not possible to decide whether they were due to creep or to the preparation of the TEM specimen.

5. DISCUSSION

The creep tests discovered a relatively large scatter of material behaviour which may be due to microstructural and chemical differences between the specimens. It was necessary to repeat the experiments five times for each test condition. By a statistical treatment of the results a good interpretation of material behaviour was possible.

The SiSiC material tested in the preoxidized state showed no significantly different mechanical behaviour from that in the as-received state. Therefore SiSiC can be regarded as a ceramic, the mechanical properties of which are not sensitive to oxidation. This fact makes discussion of the results easier. The creep curve of SiSiC was found to be well described by eqn (6).

The steady-state component, $\dot{\varepsilon}_s t$, was calculated only for Material 1 under all test conditions. In Material 2, with a much better microstructure, steady-state creep occurred only under very severe test conditions. Thus, creep of SiSiC may be regarded as being of a transient nature in general. By neglecting $\dot{\varepsilon}_s$ in eqn (6), differentiation with respect to time provides:

$$\dot{\varepsilon}(t) = m\beta\left(\frac{t}{t_0}\right)^{(m-1)} \tag{8a}$$

Equation (8) is of the same form as the more frequently used function for the description of transient creep:

$$\dot{\varepsilon}(t) = a\left(\frac{t}{t_0}\right)^{-c} \tag{8b}$$

with $c = (1 - m)$. In the case of $c = 1$, eqn (8) converts into the function of logarithmic creep:

$$\varepsilon(t) = a \ln\left(\frac{t}{t_0}\right) \tag{9}$$

Equation (9) has the disadvantage of unrealistic negative strain in the range $0 < (t/t_0) < 1$ and an infinite strain rate at the beginning of the creep test $(t \to 0)$. These disadvantages disappear when eqn (9) is written in the form:

$$\varepsilon(t) = a \ln\left(\frac{t}{t_0} + 1\right) \tag{10}$$

For long periods of times, eqn (10) converts into eqn (9). At $t =$ zero we obtain zero strain and the strain rate $\dot{\varepsilon}(t = 0) = a/t_0$.

Logarithmic creep indicates strain-hardening processes which can be described by an extended Norton creep law as follows:

$$\dot{\varepsilon} = A\sigma^n = A_0 \, e^{-B\varepsilon}\sigma^n \tag{11}$$

In this equation A_0, B and n are constants and the structure parameter A depends exponentially on the strain itself. For homogeneous stress distribution (i.e. in tension test) integration by time leads to:

$$\varepsilon(t) = \frac{1}{B} \ln (BA_0\sigma^n + 1) \tag{12}$$

Equation (12) shows the same form as eqn (11) with $a = 1/B$ and $t_0 = 1/(BA_0)$. This derivation indicates the relationship of logarithmic creep with the transient creep according to eqn (8) and therefore the mechanisms may be discussed in the same manner.

Logarithmic creep was found in metals at very low temperature where recovery processes do not occur. Deviations from this creep behaviour are known in the literature as hyperbolic creep ($c > 1$) and parabolic creep ($c < 1$).[18] In metals logarithmic creep was interpreted as increasing activation stress for dislocation motion. However, in ceramic materials this consideration is not realistic because dislocation motion does not seem to be the mechanism controlling the deformation. SiSiC consists of very stiff and less deformable silicon carbide grains embedded in the ductile silicon phase. In the undeformed material there exist a number of contacts between the silicon carbide grains. Carter and co-workers[13] investigated the SiC–SiC contacts by TEM and found no free silicon within these contacts. During creep new contacts are generated and the total area of contacts becomes larger because of local plastic deformation in the silicon carbide grains at high stress concentrations. This results in a hardening effect and also in a material behaviour dependent on strain, which may be described by a function similar to eqn (11).

The mechanisms may be discussed by regarding the microstructure in Figs 8 and 9. Before creep only a few dislocations were found in the silicon carbide and in the silicon phases. After creep the dislocation configuration in the silicon carbide phase had not changed, but in the free silicon the number of dislocations and twins increased significantly. Thus, the creep deformation of the silicon phase is controlled by dislocation motion, which is consistent with results given in the literature, where it is shown that deformation of silicon is controlled by dislocation glide. Diffusion-controlled dislocation motion was not found in silicon at temperatures up to near the melting point.[19,20]

Consequently, the strain hardening of SiSiC is not caused by the silicon phase but by the silicon carbide skeleton. The mechanisms may be deformation processes in the volume of the silicon carbide grains caused by dislocation motion or by diffusion processes and resulting in an increase of the summarized contact area. Another hardening mechanism may be the rearrangement of silicon carbide grains, resulting in a stiffer silicon carbide

skeleton. Substantial dislocation motion in silicon carbide is only possible at temperatures above 2000 °C;[21,22] thus, only local deformation by dislocation motion at highly stressed contacts may be possible. In the same way the possibilities for diffusion processes are only limited because the test temperature was approximately half of the melting point of silicon carbide (3100 K). Regarding the local stress concentration at the contacts of silicon carbide grains, both mechanisms should be possible. Nevertheless, they do not allow a large deformation of SiSiC without damage of the microstructure. The free silicon does not control the deformation because it is very easy to deform at the test temperature.[23]

The interpretation of the stationary strain component according to eqn (6) is somewhat difficult. The stress exponent of Material 1, according to the classical Norton creep law ($\dot{\varepsilon}_s = \text{const} \times \sigma^n$), was found to be $n = 5$ (Fig. 5). Such n-values are usually correlated with diffusion-controlled dislocation motion. Such a creep mechanism, however, cannot be realistic for SiSiC as shown above. Another possible interpretation is damage to the microstructure. In Fig. 9 the formation of microcracks is shown. The formation of cavities and microcracks leads to the lowering of the Young's modulus and therefore to an additional strain component.

Such a steady-state deformation process does not seem to be controlled by processes being in equilibrium. When the deformation is associated with continuous damaging the resulting creep rate in general should not be constant with time. However, an additional 'deformation' process occurs which may change or even terminate the declining character of the creep curve. At a certain time quasi-steady-state creep may emerge.

The responsible damaging may be regarded as a two-step process. The first step is the microcrack nucleation, which has been correlated to a nearly constant strain rate; the second is microcrack growth leading to an increasing strain rate. Hasselmann *et al.*[24–26] calculated the stress exponent for this so-called 'elastic creep' to be $n > 3$. Therefore the stress exponent calculated in Fig. 5 may be interpreted by the formation and later growth of the microcracks, the latter probably leading also to the formation of creep porosity, arranged in planes perpendicular to the direction of the tensile stress (Fig. 8), and resulting in an increasing strain rate with the possible consequence of creep rupture.

The question arises as to whether or not a threshold stress for initiation of the formation and growth of microcracks exists. For Material 2 stationary strain components could only be calculated at nominal stresses above 220 MPa. By looking at Fig. 7 a threshold stress becomes more clear. The significant increase of strain above 200–220 MPa should be interpreted by microcrack formation and crack growth activated above this stress. From Fig. 7 it is also seen that the threshold stress shifts to lower values when the

time for which the strain is taken is increased. The processes leading to crack initiation and growth are therefore stress- and time-dependent.

When a critical stress concentration in the silicon carbide structure is needed for crack initiation and growth, its time dependency can be explained as follows. At the beginning of bending creep possibilities for local deformations and rearrangement of silicon carbide grains exist and the critical stress concentration will not be reached at any silicon carbide contacts in the specimen. With increasing time the initial deformation mechanism will be blocked more and more (strain hardening). The stress concentrations increase and may perhaps reach the critical value at one of the silicon carbide silicon carbide contacts. A crack will be initiated and at this contact the stress concentration decreases. So, the microcrack will not propagate at first and the stress concentration increases at other silicon carbide -silicon carbide contacts.

Therefore, to reach higher stress concentrations a certain deformation by creep is needed. The time necessary for this process is shorter, the higher the nominal stress. The time for reaching the critical stress concentration may be correlated with the incubation time for reaching higher strain values in Fig. 7.

By this procedure the silicon carbide structure will be weakened more and more, and after a certain time the microcracks will begin to grow and contribute to the creep porosity shown in Fig. 10 and also to strain. The time at which microcrack growth occurs may be regarded as stress-dependent; thus, the shifting of the threshold stress to lower values in Fig. 7 may be explained.

6. CONCLUSION

Reaction-bonded siliconized silicon carbide with a well-defined microstructure shows a very good creep behaviour that is not sensitive to severe oxidation treatment. The creep is of a transient nature and can be described by an extended Norton creep law considering the strain-hardening behaviour of the material. The deformation of SiSiC is controlled by the silicon carbide skeleton, while the free silicon is very ductile and easy to deform under the applied test conditions. Small local deformations of the silicon carbide grains by dislocation motion or diffusion processes are responsible for the transient creep. Also, some rearrangement of the silicon carbide grains may be possible. These processes cause the strain hardening. The total deformation that can be reached without disturbance of the microstructure is very limited. Steady-state creep components occur only at high stress levels, creating microcracks and creep porosity within the

microstructure. Creep rupture occurs only above a threshold stress and is due to the growth of microcracks at high stress concentrations.

REFERENCES

1. Marshall, P., The relationship between delayed fracture, creep and texture in silicon carbide, *Special Ceramics*, **4** (1967) 191–203.
2. Rumsey, J. C. V. and Roberts, A. L., Delayed fracture and creep in silicon carbide, *Proc. Brit. Ceram. Soc.*, **7** (1967) 233–45.
3. Marshall, P. and Jones, R. B., Creep of silicon carbide, *Powder Metallurgy*, **12** (1969) 193–208.
4. Adams, R. M., The creep of silicon carbide; its measurement and mechanisms, Ph.D. Thesis, University of Leeds, 1972.
5. Osborne, N. J., Creep testing of high temperature engineering ceramics, *Proc. Brit. Ceram. Soc.*, **25** (1975) 263–80.
6. Seltzer, M., *High Temperature Creep of Ceramics*, Rept. No. AD-A 031 760, 1976.
7. Krishnamachari, V. and Notis, M. R., Interpretation of high temperature creep of SiC by deformation mapping techniques, *Mat. Sci. Eng.*, **27** (1977) 83–8.
8. Larsen, D. C., Borth, S. A., Ruh, R. and Tallan, N. M., Evaluation of four commercial Si_3N_4 and SiC materials for turbine application, in *Ceramics for High Performance Application II*, Eds J. J. Burke, E. N. Lenoe and R. N. Katz, Brook Hill, Chestnut Hill, Massachusetts, 1978, 651–67.
9. Wirth, G., Gephart, W. and Schönau, W., *Zug- und Biegekriechverhalten sowie Biegebruchfestigkeit von HP- und RB-Silizium-Karbid bei hohen Temperaturen an Luft*, DFVLR-Bericht IB 354-78/3, 1978.
10. Schnürer, K., Kriechverhalten verschiedener SiC-Materialien im Vakuum und an Luft, Dissertation Universität Karlsruhe, 1979, KfK-Bericht 2883.
11. Schnürer, K., Grathwohl, G. and Thümmler, F., Kriechverhalten verschiedener SiC-Werkstoffe, *Science of Ceramics*, **10** (1980) 645–52.
12. Gugel, E., Leimer, G., Cohrt, H., Grathwohl, G. and Thümmler, F., Gasturbinenbauteile aus reaktionsgesintertem SiC und deren mechanische Hochtemperatureigenschaften, in *Keramische Komponenten für Fahrzeug-Gasturbinen II*, Eds. W. Bunk and M. Böhmer, Springer-Verlag, Berlin, 1981.
13. Davis, R. F., Carter, C. H. Jr, Chevacharoenkul, S. and Bentley, J., The occurrence and behavior of dislocations during plastic deformation of selected transition metal and silicon carbides, in *Deformation of Ceramic Materials II*, Eds R. E. Tressler and R. C. Bradt, Plenum Press, New York, 1984.
14. Cohrt, H., Grathwohl, G. and Thümmler, F., Non-stationary stress distribution in a ceramic bending beam during constant load creep, *Res Mechanica*, **10** (1984) 55–71.
15. Andrade, C., On the viscous flow in metals and allied phenomena, *Proc. Roy. Soc.*, **A84** (1911) 1–12.
16. Cottrell, A. H. and Aytekin, V., Andrade's creep law and the flow of zinc crystals, *Nature*, **160** (1974) 328–9.
17. Cohrt, H., *Mechanik und Mechanismen des Biegekriechens von reaktionsgebundenem Siliziumkarbid*, KfK-Bericht 3731, 1984.

18. Seeger, A., Theorie der Kristall-Plastizität, *Z. Naturforschung*, **9a** (1954) 758–75.
19. Reppich, B., Haasen, P. and Ilschner, B., Kriechen von Silizium-Einkristallen, *Acta Met.*, **12** (1964) 1283–8.
20. George, A., Escaravage, C., Champier, G. and Schröter, W., Velocities of screw and 60°-dislocation in silicon, *Phys. Stat. Sol. (b)*, **53** (1972) 483–96.
21. Frantsevich, I. N., Kravets, V. A., Egorov, L. O., Nazarenko, K. V. and Smusherich, V. S., High-temperature deformability of α-SiC, *Soviet Powder Metallurgy*, **10** (1971) 229–31.
22. Frantsevich, I. N., Kravets, V. A. and Nazarenko, K. V., Investigation of α-SiC plastic strain, *Poroshkovaya Met.*, **15** (1975) 89–93.
23. Sylwestrowicz, W. D., Mechanical properties of single crystals of silicon, *Phil. Mag.*, **7** (1962) 1825–45.
24. Hasselmann, D. P. H., Venkateswaran, A. and Shih, C., Elastic creep of brittle ceramics with special reference to creep by crack growth in aluminium oxide, in *Surfaces and Interfaces in Ceramic and Ceramic–Metal Systems*, Eds J. A. Pask and A. G. Evans, Plenum Press, New York, 1981.
25. Venkateswaran, A. and Hasselmann, D. P. H., Elastic creep of stressed solids due to time dependent changes in elastic properties, *J. Mat. Sci.*, **16** (1981) 1627–32.
26. Hasselmann, D. P. H. and Venkateswaran, A., Role of cracks in the creep deformation of brittle polycrystalline ceramics, *J. Mat. Sci.*, **18** (1983) 161–72.

Received 29 May 1985; accepted 15 July 1985